5. Orogen-wide patterns of strain accumulation – the Andean case

To better understand and quantify deformation frameworks on multiple spatial and temporal scales, the attempt is often made to find scaling laws of strain accumulation for the comfortable extrapolation of data to all scales. However, scale invariance vs. characteristic lengths of structures and deformation in stages has not yet been studied in detail on the orogen scale in relation to the next smaller regional scale. By means of (geo)statistical methods we examine the strain evolution on the orogen scale for the Central Andean plateau (17-27°S and ~69-63°W) for the last 46 Ma based on a comprehensive literature compilation of all available deformation data. Thus, we are able to detect typical lengths of structures and characteristic temporal patterns of strain accumulation on both the regional and the orogen scale. Regionally active areas commonly have widths of 150-200 km and along-strike extents of 200-300 km. On the orogen scale however, they are coevally active over lengths of 600-800 km. This is true for all deformation stages which are typically 2-4 Ma long. Therefore, we propose the following temporal pattern for the Central Andean plateau, which is refined compared to previous estimates: 46-43 Ma, 42-41 Ma, 40-34 Ma, 33-29 Ma, 28-18 Ma, 17-13 Ma, 12-11 Ma, 10-9 Ma, and 8 Ma to present.

5.1. Introduction

Extensive work has been done to detect critical scaling laws that relate e.g., the frequency of seismic events with their magnitudes (Gutenberg-Richter, e.g., Bak and Chang, 1989; Kagan and Jackson, 1991; Bak, 1996), the displacement of faults with their length (e.g., Watterson, 1986; Walsh and Watterson, 1988; Sornette and Davy, 1991; Dawers and Anders, 1995; Wojtal, 1996; Nicol et al., 1996), the length of a fault with its slip frequency (Scholz et al., 1993; Bellahsen et al., 2003), or the length of fault segments with their frequency (Okubo and Aki, 1987; Wojtal, 1994). Such scaling relations follow power laws that are practically valid on all scales, so that data from one scale could be extrapolated to another, e.g., bigger scale like the orogen itself, which cannot easily be studied in detail.

However, not all deformation processes underlie this “fractal” deformation framework, but rather follow the continuum-Euclidean view, in which strain localizes along some faults or fault systems (strain weakening); or the granular view, in which strain accumulation is diffuse (strain hardening). It has been suggested that deformation frameworks alternate over time (cf. Ben-Zion and Sammis, 2003), and characteristic patterns exist. Unfortunately, characteristic structures superpose each other, so that they can hardly be attributed to the respective deformation framework and thus, deformation patterns cannot easily be detected in the field. In addition to this difficulty, temporal patterns on one spatial scale need not be the same on another, unless strain accumulation was scale-invariant.

In this study we aim to examine the strain pattern on the orogen scale for the Central Andean plateau (17-27°S and ~69-63°W) on the base of a thorough literature compilation of all available deformation data, and to detect typical lengths of structures and characteristic duration of strain accumulation on both the regional scale (e.g., fault systems and networks) and the orogen scale by means of (geo)statistical methods. By comparing the two, we are able to examine the effect of spatially smaller scales on the next bigger scale over time, and to elaborate on the permissibility of extrapolating data from one scale to another.

5.2. Geological setting

The Central Andes are the result of the last ~46 Ma of subduction of the oceanic Nazca plate beneath the South American continent, and bear one of only two active plateau orogens worldwide. The studied region comprises four major units (excluding the fore-arc region), which are from west to east: a. the Western Cordillera (magmatic arc), b. the Altiplano plateau, c. the Eastern Cordillera, and d. the Subandean fold-and-thrust belt (cf. Fig. 5.1). This is true for the plateau north of 24°S; south of 24°S, the plateau is called the Puna.

In the Central Andes, the amount of shortening varies along-strike and reaches a maximum of 260-280 km at 21°S (summary of

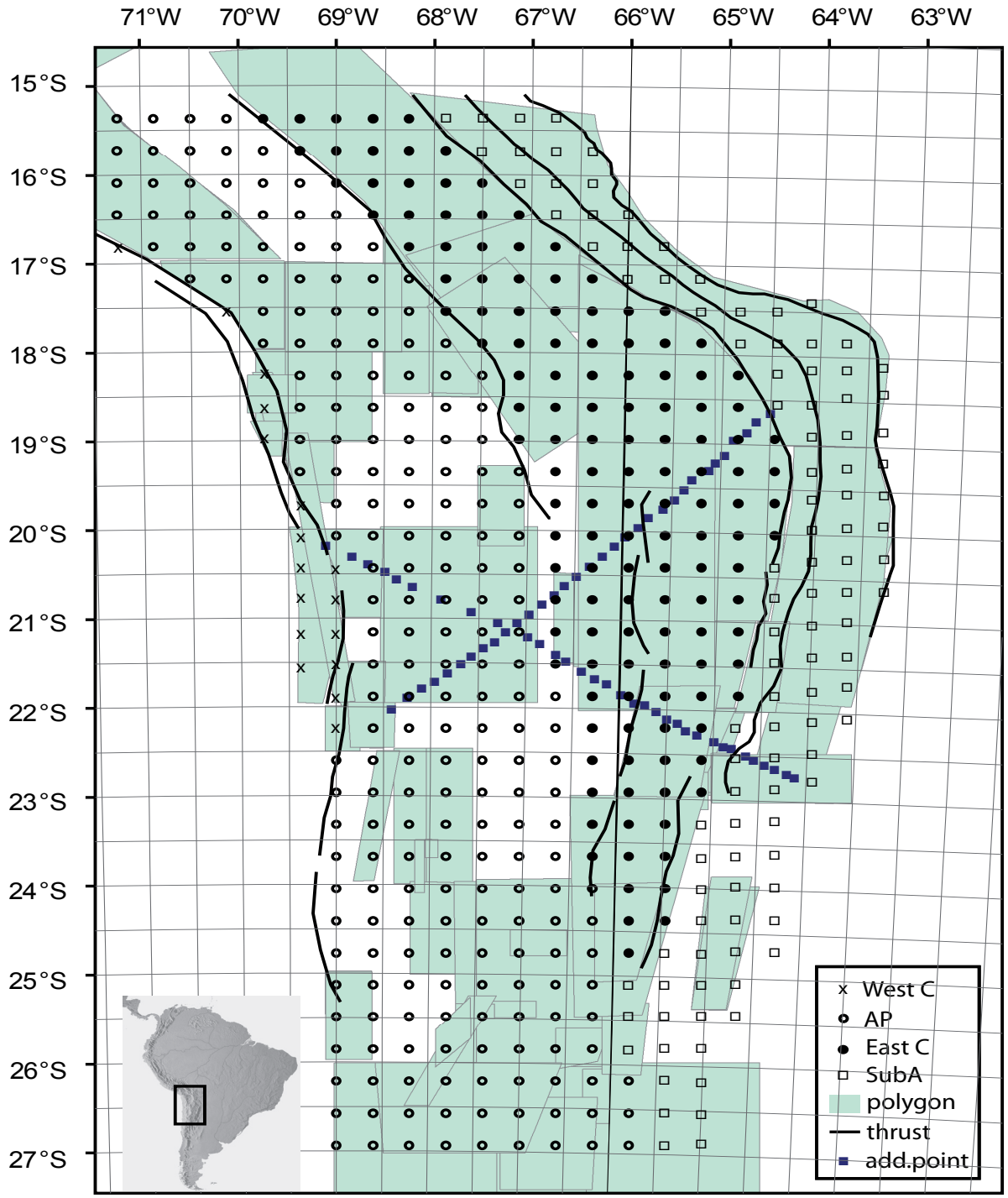

Fig. 5.1: The study area of the Central Andes comprises the four structural units from west to east, which are separated by major thrust faults (black lines): Western Cordillera (crosses), Altiplano-Puna plateau (points), Eastern Cordillera (solid points), and Subandean fold-and-thrust belt (squares). Each of these points is part of the point grid that overlies the polygons (grey area), for which deformation data are given. Areas for which no appropriate data exist are left white. To the lower left a small map of South America shows the location of the study area (black box).

shortening estimates in Oncken et al., 2006). Deformation has commonly been divided into three main orogenic pulses (45-30 Ma, 30-10 Ma, and 10-0 Ma) of which each has an established shortening rate (0-8 mm/yr; 6-10 mm/yr; and 8–14 mm/yr respectively with 9-15 mm/yr as the present-day value, summary in Oncken et al., 2006). Due to numerous datable syntectonic deposits like volcanic ash horizons and little erosion, the deformation activity in the Central Andes is highly resolved both in space and time.

On the basis of a thorough literature compilation of all available deformation data, Oncken et al. (2006) were able to refine these pulses into five main deformation stages (46-37 Ma: deformation in both Cordilleras; 36-30 Ma:

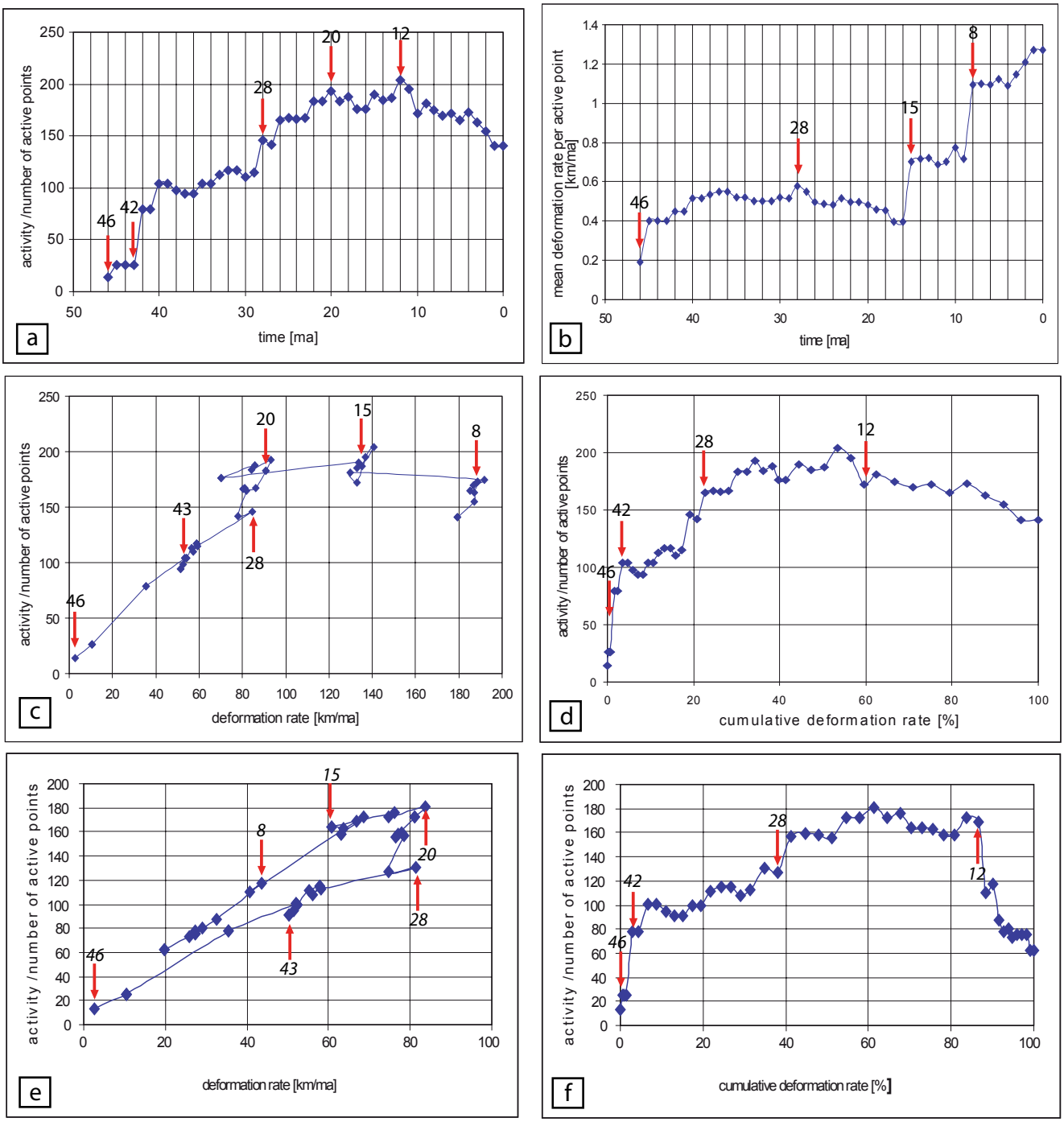

Fig. 5.2: Plots of frequency statistics, for which we mark the beginning of major deformation stages with red arrows: a. the number of active points over time shows how many points, i.e., how much of the total area has actively undergone deformation for a given million year from 46 Ma to the present; b. the mean deformation rate per point (points of all structural units) over time; c. the number of points vs. the cumulative deformation rate (in km/Ma); d. the number of points over cumulative deformation rate (in %); e. is similar to c. but without data points of the Subandean fold-and-thrust belt; and f. is similar to d. but without the Subandean. Stages inferred for e. and f. are in italics to show that the "stages" would be similar to the other stages a.-d., but they are not included in the summary.

deformation in the intramontane basin of the plateau area; also 29-20 Ma and 19-8 Ma, and 7-0 Ma: transfer of the active deformation away from the plateau into the Subandean fold-and-thrust belt). These times are characterized by coeval strain accumulation within the main structural units of the Central Andean plateau along-strike for several hundred kilometres. The authors suggest that these characteristics are only observed when deformation data are examined on time scales of >5 Ma.

5.3. Data preparation

The databank published in Oncken et al. (2006) includes a compilation of the existing literature on deformation activity for our study area for the last 46 Ma (appendix A). Each data set includes the start and end of deformation

activity in millions of years (Ma) inferred for the geographic area given with exact coordinates by the respective authors. We take into account only those references that precisely document the location of the study area, the position and processing of samples, and the used method for dating. We further weight the data according to the accuracy of the sample coverage (e.g., how many samples, dating error), the number of available references for an area, and the age of publication. The data cover almost the entire area, except for some regions within the Altiplano (between 18.5-19.5°S and 22.5-23.5°S) for which the field exposure is not good for deformation quantification.

All data were then plotted as deformation polygons in an ArcGis project, as given by the geographic coordinates of the study areas (Fig. 5.1). Each polygon has been attributed the start and end of deformation. Instead of continuing the analysis with irregularly shaped polygons, we convert the data into a regular grid of points (spacing is 40 km). We chose this distance as the smallest study areas given from literature have widths of slightly more than 40 km, which still allows two grid points to be located within it. However, most study areas are several hundred kilometers in length, for which there is no variation between the grid points. Therefore, a higher resolution, i.e., a smaller distance than 40 km between grid points is not useful. To cover the values below the grid steps for geostatistical analysis, it is common practice to include some additional points with a smaller but random distance.

Next, each of these points is assigned the information of the polygon in which it plots, namely the geographic coordinates (x, y), the start and end of deformation, and the respective structural unit of the Central Andes in which the point is located. In case a point plots in several polygons, it is assigned the information of each.

5.3.1. Deformation activity

As we know the beginning and end of deformation for each point, we can calculate the duration of deformation activity for each point. For each time step of 1 Ma out of the 46 million years, we assign every point either activity for a given Ma (nominal value of 1), or inactivity for a given Ma (value is 0). We chose time steps of 1 Ma as the error for the deformation ages are commonly on the order of 1 Ma. Therefore, it does not make sense to use smaller time steps, which are not reliable due to this constraint. The resulting data set of deformation activity includes a total of ~440 nominal values of 0 and 1.

5.3.2. Shortening rates

Additionally, we determined the shortening rate for each point of the grid (or deformation rate). Oncken et al. (2006) compiled published shortening estimates inferred from balanced cross sections, which exist for all latitudes of the study area and in between; and mostly include estimates for each of the structural units individually. The amount of shortening known from this compilation is divided by the number of points that lie in the respective balanced cross section according to our grid. This gives us the shortening estimate for an area that is located between two neighbouring points. As we also know how long each point was actively deforming, we can further divide these estimates by the duration of deformation and obtain shortening rates. Shortening rates for small areas (40 km) for 1 Ma tend to be rather low compared to big areas, and therefore strain rates would be better as they can be used irrespective of the initial length. As we do not know the initial length of each of the 40 km areas, we cannot calculate strain rates.

We acknowledge that this procedure is only valid under the assumption that strain accumulates homogeneously and if all faults in a polygon have equally accommodated strain. We will discuss this issue at a later stage.

5.4. Statistics

For the frequency statistics, different deformation times are differentiated according to breaks in lines from one million year to the next million year, when one of the following criteria is met: 1. the number of active points changes by ~50 or more, 2. the difference in nominal values between two points makes up ~50% of the smaller value or more, or 3. the slope of the curve from one point to the next is higher than ~60° (i.e., increase of the nominal values when the slope goes up, or decrease when the slope goes down).

For the geostatistics, temporal patterns are differentiated when a spatial variation of the data exists from one million year to the next, depending on 1. the value of variation, 2. the direction of highest variation, or 3. the characteristics of the sill (i.e., highest value of variation), the range (i.e., the distance beyond which the variation becomes

stable) or the hole effect (which indicates a correlation between points at a higher distance). All of these characteristic features are further described below. We also carried out a sensitivity analysis (cf. section 5.5.1. and Appendix A), in which we weighted the significance of each of the time steps.

5.4.1. Frequency of deformation activity

We plotted the frequency of deformation activity of all units against time, i.e., the number of active points for each million year (Fig. 5.2a). Depending on the breaks of the line, the following deformation stages can be detected: 46-43 Ma, 42-29 Ma, 28-21 Ma, 20-13 Ma, and 12-0 Ma.

5.4.2. Frequency of shortening rates

We plot the mean shortening rates (i.e., for distances of 40 km) for each Ma, which is a value averaged for all points over all structural units (Fig. 5.2b). Another plot includes the number of active points vs. the cumulative deformation rate, which shows how much area is involved in each 1 Ma to account for the given deformation rate (values in Fig. 5.2c include all structural units, whereas Fig. 5.2e excludes the Subandean fold-and-thrust belt). When two consecutive points are far apart and its slope is zero or negative, the shortening rate per point has increased from one million year to the next (as fewer points are active). On the other hand, if the slope increases, more points have become active suggesting that the shortening rate decreases for each point. When figures 2c) and 2e) are compared, it becomes obvious that when the Subandean is not included in the plot (Fig. 5.2e), the deformation rate decreases drastically for the last 15 Ma, as the fold-and-thrust belt in the Interandean/ Subandean has accumulated most of the shortening for the last 15 Ma. This can also be seen in figures 5.2d) and 2f), which depict the number of active points over the percentage of cumulative deformation rate, again for all units and without the Subandean respectively.

In general, each of the following times indicates the beginning of a deformation period: 46 Ma, 43 or 42 Ma, 28 Ma, 20 Ma, 15 or 12 Ma, and 8 Ma.

Figure 5.3 shows data for each of the structural units individually, namely the deformation rate and the mean deformation rate per active point over time. Thus we can detect characteristic patterns of each structural separately. In figures 5.3a) and b) it becomes clear, that the Western Cordillera is active from 46-38 Ma with very low shortening rates, after which strain accumulation in the Western Cordillera practically ceases.

The Altiplano plateau (Fig. 5.3c-d) shows dominant deformation activity between 33-12 Ma for which the shortening rate constantly increases. The mean deformation rate per active point however experiences fluctuations with an increase from 33-27 Ma, and a subsequent decrease to a lower but constant value.

The Eastern Cordillera (Fig. 5.3e-f) shows a constant deformation rate from 40-29 Ma, followed by a peak at 28 Ma and a subsequent steady decrease until 17 Ma, with another drastic decline until 10 Ma, after which the shortening rate is comparatively small. Similar fluctuations can be observed for the mean deformation rate per active point.

In contrast, the fold-and-thrust belt does not accumulate shortening in the Interandean until after 15 Ma, and in the Subandean until after 10 Ma.

5.4.3. Other patterns

Figure 5.4a shows the deformation rate for each point of the grid averaged over the last 46 Ma. In general one can say that the Western Cordillera has the lowest shortening rates, followed by the plateau area that has also experienced lower deformation rates than the Eastern Cordillera and the Subandean. The latter two structural units have lower shortening rates towards the northern and southern boundaries of the study area, which can be explained by the oroclinal bend.

Figure 5.4b shows the duration of deformation activity for each point of the grid. Except for the Subandean belt, there is a correlation between the duration and the deformation rate: the higher the deformation rate for an area, the longer it was active. This correlation is partly due to the assumption of homogeneity, which was necessary to obtain shortening rates (cf. section 5.3.2.).

5.4.4. Geostatistics

Variogram analysis is a common method to analyse the variation (i.e., the inversion of correlation) of a variable in a temporal, spatial, or spatiotemporal context (e.g., Matheron, 1962; 1970; Journel, 1977; Deutsch and Journel, 1992). The variable is defined by spatial coordinates (x, y) and a nominal value. Variogram analysis

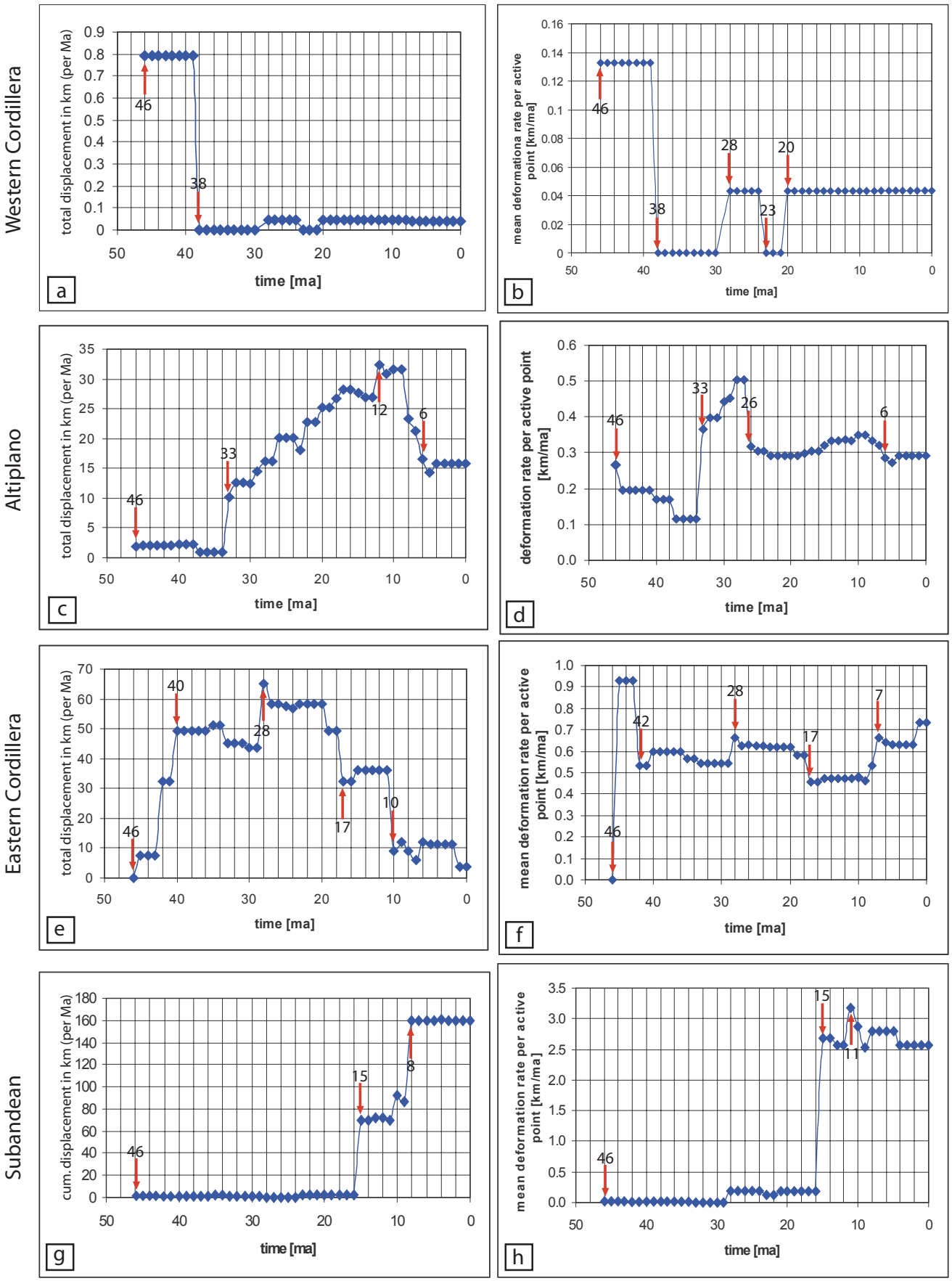

Fig 5.3: Plots of frequency statistics for each of the four units (arrows mark the beginning of major deformation times), namely the displacement over time (left column) and the mean deformation rate per active point over time (right column).

can only be implemented when the variable is continuously distributed in space. This is true for both deformation activity, which is either 0 or 1 at every location, and shortening rate, which is 0 or a

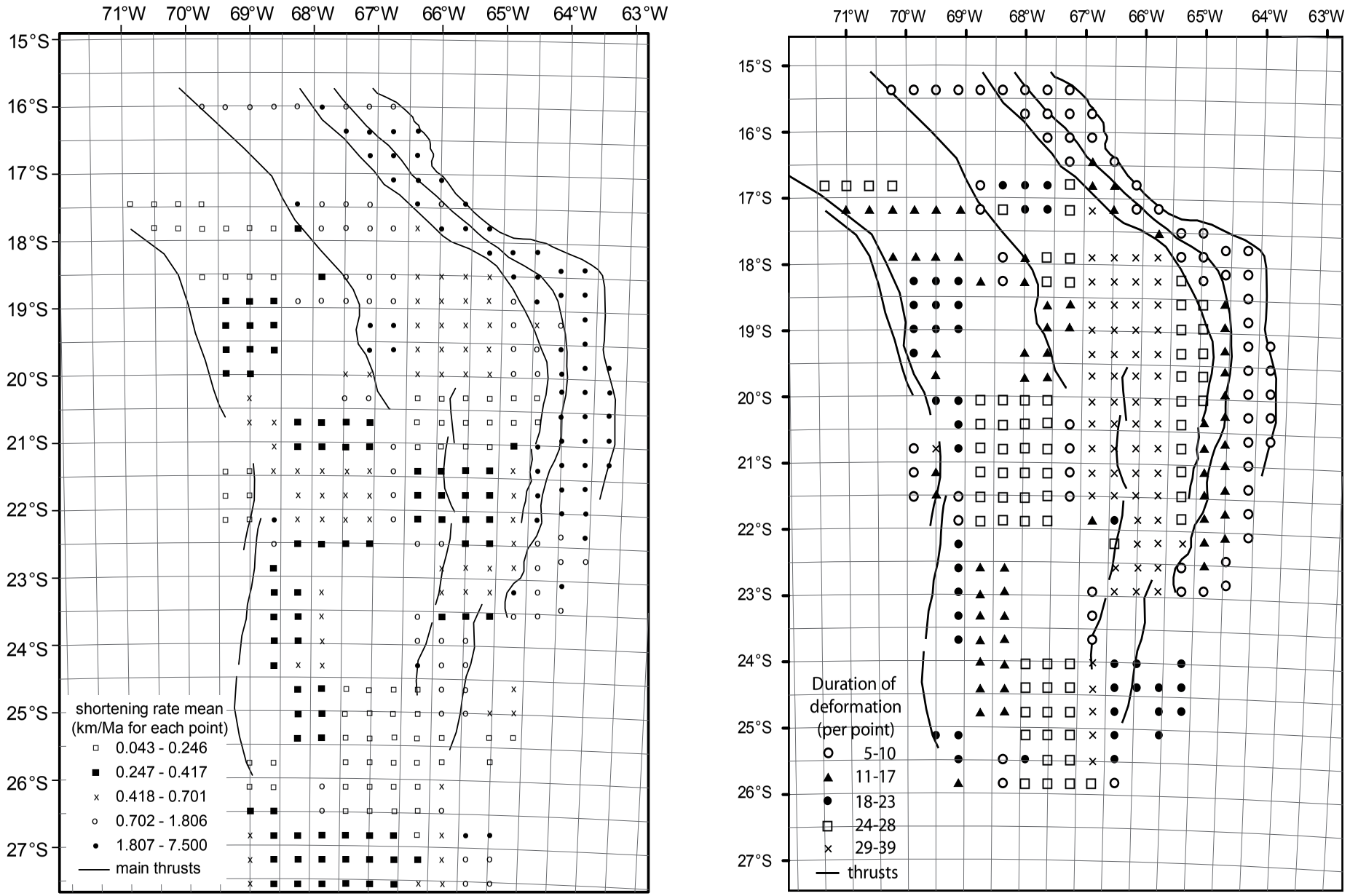

Fig. 5.4 a (left), b (right): The points carry information on their a) mean shortening rate in km/Ma and b) duration of deformation in Ma (refer to legend for nominal values). The values in a) represent the average over 46 Ma, yet there is a clear difference in values over the structural units.

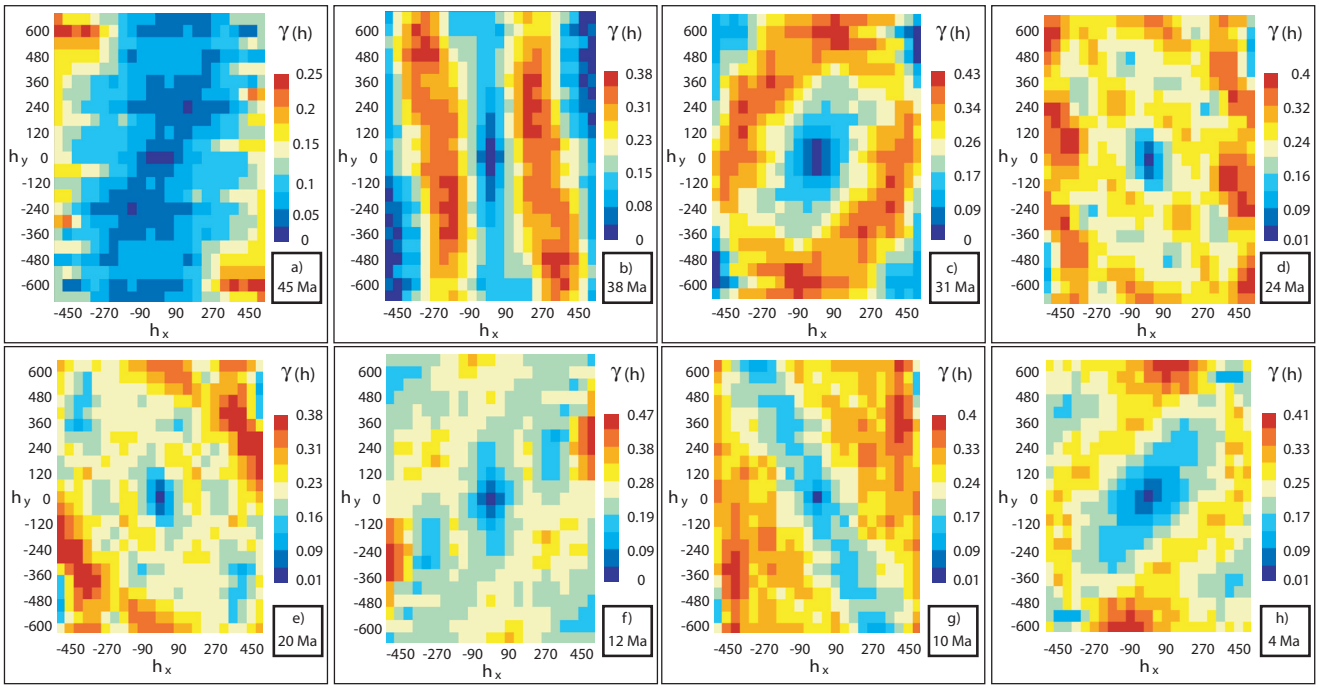

Fig. 5.5: Indicator variogram surfaces are shown for eight different time windows (1 Ma), each representing the spatial variation of deformation activity for a significant deformation period. The data are described in more detail in-text.

positive integer. The main objective of the analysis is to calculate the differences in value of the variable at spatial positions that are separated by a distance "h". This difference between values is calculated for all possible "h" and in all possible directions, and forms the major part in the formula of variation with $z(x_i)$ and $z(x_{i+h})$ being the values of the variable at position (x_i) and (x_{i+h}) respectively, N (h) is the number of pairs of points (x_i and x_{i+h}) that are separated by a distance h (in km):

For example, if we have one active area of the extent "y", then "h" will be low for all h<y,

$$\gamma^*(h) = \frac{1}{2\,N(h)} \sum_{i=1}^{N(h)} \left[z(x_i) - z(x_i + h) \right]^2$$

as then the distance is calculated for two points that are both located within the same deformation area. For larger ranges "h" between two points, the points are likely to fall within different deformation areas, or one is active and the other is not, and the variation becomes higher. The advantage of the method is its ability to a. quantify the degree of spatial correlation of strain accumulation (e.g., over the entire orogen vs. the next smaller scale) for a given direction, also b. in a temporal context. Thus, it enables us to detect scale invariance vs. characteristic lengths of actively deforming regions and correlation of different structural units.

5.4.4.1. Indicator variogram surfaces

Indicator variogram surfaces are maps of the spatial variation of a variable (Fig. 5.5). The variation is colour coded, and is given for all distances "h", namely for both positive and negative x-directions (h_x) and y-directions (h_y). Thus, the spatial position is not directly given in geographic coordinates, but via the distances "h" (in km) between geographic coordinates. This is the reason why the variation is point-symmetrical about the origin in the center of each map (Fig. 5.5). The pattern of these maps indicates the directions of anisotropy, i.e., the direction for which the minimum and maximum variation is most persistent in space. The maximum extent of the active areas can be identified from the maps when clear anisotropy directions are present. For Fig. 5.5b) this is 200 km in width and 600 km in length, for Fig 5.5c) about 400 km both in width and length, for Fig. 5.5f) 200 km in width and 600 km in length, for 5.5g) 200 km in width and 600 km in length, and for Fig. 5.5h) 200 km in width and up to 600 km in length. The upper cut-off is 600 km for the indicator variogram surfaces, so potential length higher than 600 km were not resolved.

The following major stages with their respective main anisotropy directions (and orthogonal to them) can be summarized (Fig. 5.5 a-h): a. 46-43 Ma (NNW-SSE), b. 42-34 Ma (N-S), c. 33-29 Ma, d. 28-21 Ma (NNW-SSE), e. 20-13 Ma (NW-SE), f. 12-11 Ma (NNE-SSW), g. 10-9 Ma (NNW-SSE), and h. 8-0 Ma (NE-SW).

5.4.4.2. Indicator variograms

Indicator variograms (Fig. 5.6) are another way of depicting the spatial variation of the variable. The distance "h" between two points (x-axis) is plotted against the variation of deformation (y-axis). The resulting curves have several characteristic features. The distance "h", for which the curve does no longer increase, which means that there is no more variation for larger "h", is called the "range". Beyond the range, the value for variation remains stable and is called the "sill". A third characteristic feature of variograms is the "hole effect", occurring when the curve slopes down (i.e., decreases in variation) to increase in slope again (i.e., increases in variation) with higher "h". Such hole effects are present, e.g., when a small inactive deformation area is embedded between two actively deforming areas. Thus, the active areas would have a "hole" of inactivity in between. Variograms can include all directions at once (omnidirectional), or a range of specific directions, which are given by numbers: 0 indicates E(ast), 90 is N(orth), 180 is W(est) and so on. In Figure 5.6, we can differentiate the following significant time windows with average extents of actively deforming areas (e.g., the range commonly indicates the minimum extent of an active area as the sill becomes stable, i.e., no more variation occurs for longer ranges "h", which is the maximum extent):

a) The first stage 46-43 Ma is determined by the omnidirectional variogram, as only few points are active. This is also the reason for the low value of the sill (~0.1), which means that almost no variation is present for either small or large distances "h". A range of about 90 km can be inferred from the first slope, which decreases thereafter to increase again slightly after ~450 km. The first value reflects the width of the active units, the second gives their maximum along-strike extent. The sill is stable at 200 km, which indicates the general length of the active units.

b) The stage between 42-34 Ma has a clear anisotropy along-strike of the units, namely to ENE-WSW (20) and perpendicular to it NNW-SSE (110). In the first anisotropy direction, the range yields ~200 km reflecting the maximal width of the active units. A hole effect is present between 400 km and 750 km in the same direction. This explains that inactive areas can be found in between active areas. In the second direction, no more variation exists beyond the range of ~200 km, which means that the along-strike extent of deformation areas is 200 km or larger (for which case there is no more variation within one deformation area), and can be active along-strike for up to ~800 km.

c) Stage 33-29 Ma is characterized by deformation within the center of the study area (namely Eastern Cordillera and Southern Altiplano). The variation is similar in all directions for the same distances "h". The inferred range of ~400 km reflects the maximum diameter of a continuously active area. A hole effect between 400 and 800 km is related to the regions beyond this active area up to the boundaries of the study area.

d) Stage 28-21 Ma has no clear anisotropy in any direction, because the active areas are partly turning around the oroclinal bend. However, a range of 180-270 km in the E-W direction reflects the E-W extent of the active areas. The strong hole effect at 600 km for the E-W direction can be explained by the limited extent of the study area in this direction. The range in NNW-SSE direction is 240 km. A slight hole effect between 360 and 600 km can be attributed to the bending of some of the active areas. The maximum length of structural units beyond the hole effect is ~700 km. This illustrates the possible minimum and maximum along-strike extents of the active units.

e) Stage 20-13 Ma is similar to the previous stage, with the range for the ENE-WSW direction being ~150-200 km reflecting the widths of the active areas. The hole effect in this direction between 200 and 400 km reflects the variation between active and inactive areas perpendicular to their strike. The range for the NNW-SSE direction is at 270 km, which is the minimum length of active units along-strike. The sill is stable up to 600-800 km which is the

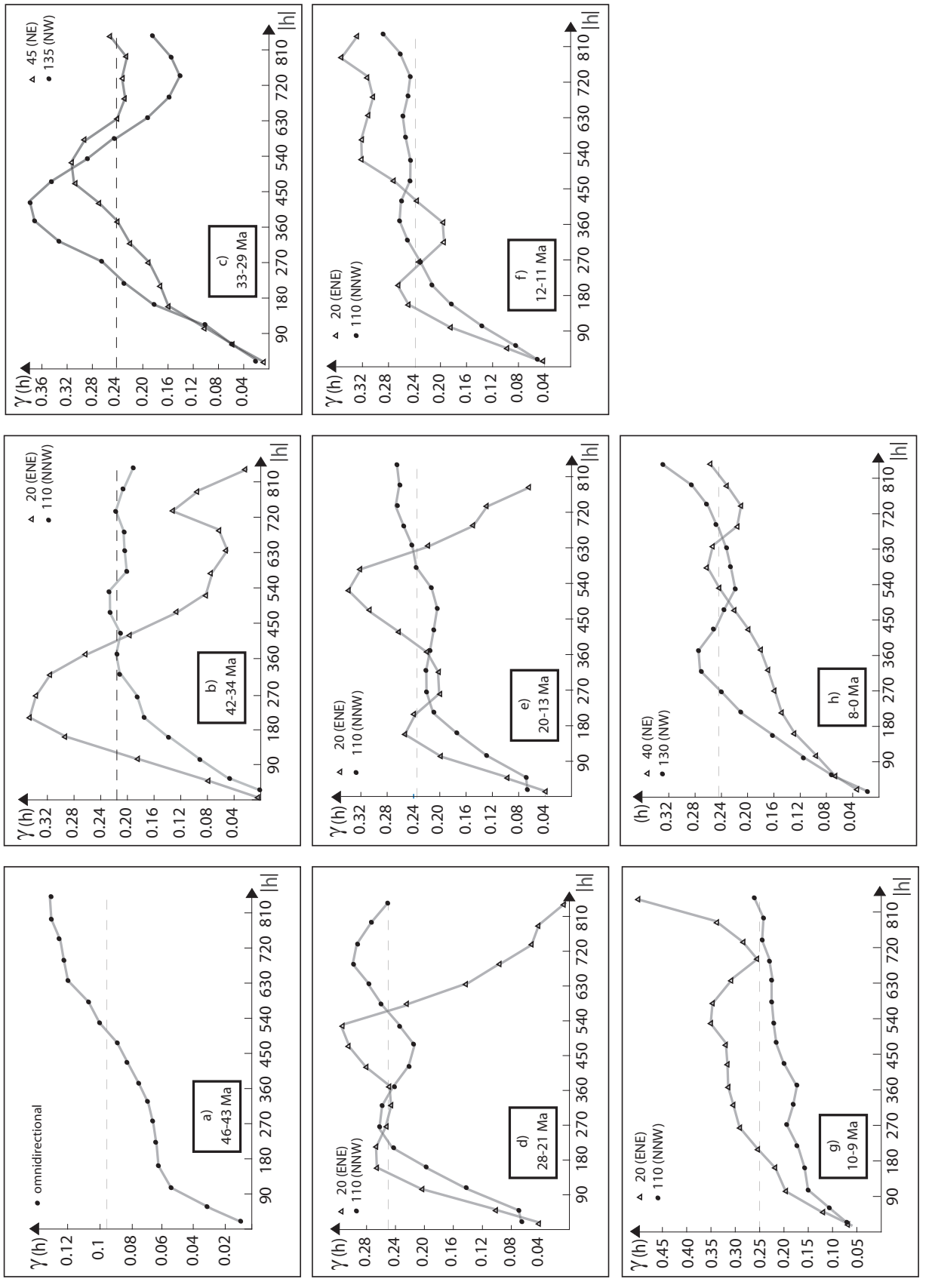

Fig. 5.6: Indicator variograms show the variation of deformation distribution (y-axis) over distances h (x-axis). Two different curves are given in parts b) to h), which represent the variation in the directions specified in the upper corner of each plot. Only a) shows an omnidirectional variogram, which means that variation was not studied in a specific direction. Further description of the plots in-text.

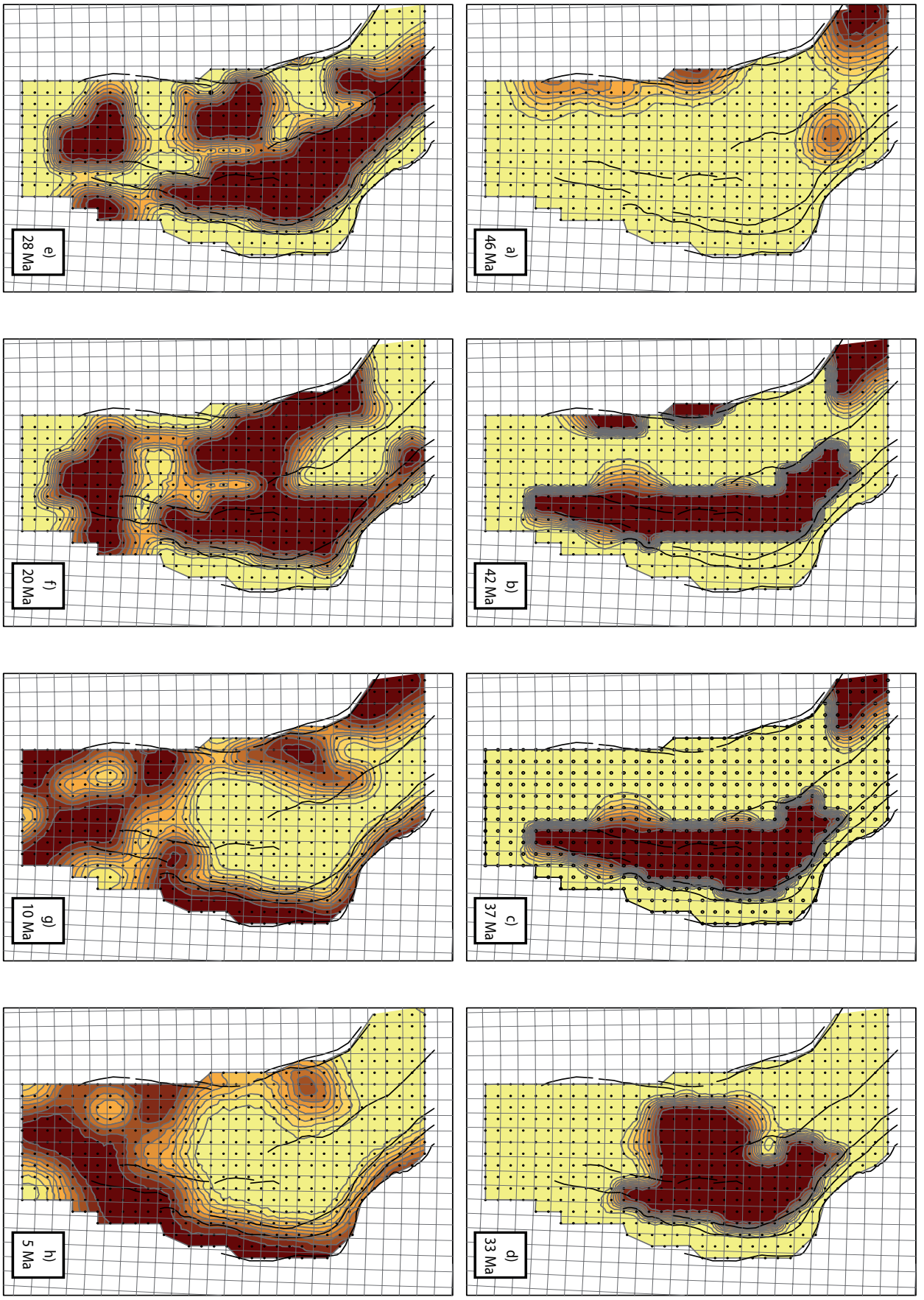

Fig. 5.7: Each of the eight maps a) to h) shows a contour plot of active deformation (brown colours) and inactive regions (yellow) interpolated by kriging. Further description of each of the plots in-text.

maximum along-strike extent.

f) Stage 12-11 Ma shows clear anisotropy directions to the NNW-SSE and orthogonal to it with ranges of ~400 km (minimum length) and ~150-200 km (width) respectively. However, active areas attain length up to 800 km. The smaller value is caused by the oroclinal bend region, which separates one long active unit into areas of different characteristic strike/ anisotropy.

g) Stage 10-9 Ma is again characterized by a slight anisotropy in the NNW-SSE direction reflecting active areas north of the oroclinal bend (namely the northern part of the Western Cordillera, the Peruvian Altiplano, and the northern Subandes). The generally low variation indicates the long spatial continuity along-strike of active units up to 800 km. The range is ~270 km indicating the along-strike extent of smaller areas. The range for the ENE direction is about 100-200 km indicating the width of the deformation areas.

h) The final stage 8-0 Ma is once more characterized by anisotropies to the NW-SE and NE-SW. The range is ~300 km in the first direction and ~150-200 km in the second. This reflects the minimum widths of the units. Active areas in the NW-SE direction attain length of up to 600 km (with a hole effect from 400 km to ~600 km, which reflects the inactive areas in between the still active margins. In the NE-SW direction, the sill steadily increases showing that active areas wider than 200 km are present.

Active areas around the oroclinal bend will not entirely be resolved in the analyzed directions. In fact, the maximum extent of ~600-800 km as in stages f), h), g) in the NNW direction can also be found in other directions, e.g., to the NW. Thus, the entire length of active areas can increase up to almost the total extent of the study area.

5.4.4.3. Kriging plots

Modelled indicator variograms are the base for kriging (e.g., indicator kriging or ordinary kriging), which are interpolation algorithms. They allow the smooth display of our point data for every million year in space. The following eight stages are most prominent (Fig. 5.7): a. 46-43 Ma, b. 42-38 Ma, c. 37-34 Ma, d. 33-29 Ma, e. 28-21 Ma, f. 20-11 Ma, g. 10-6 Ma, and h. 5-0 Ma.

5.4.4.4. Variogram surfaces: shortening rates

Similar to the diagrams in Figure 5.5, we also performed variogram analysis on the spatial variation of the shortening rate, of which eight variogram surfaces are prominent (Fig. 5.8). The following time windows can be differentiated according to the variations from one million year to the next and with their respective main anisotropy directions (Fig. 5.8 a-h): a. 46-41 Ma (NNW-SSE), b. 40-34 Ma (NNW-SSE), c. 33-29 Ma, d. 28-24 Ma (NW-SE), e. 23-18 Ma (NW-SE), f. 17-11 Ma (NNE-SSW), and g. 10-0 Ma (N-S).

5.5. Results

5.5.1. Sensitivity analysis

All inferred deformation stages from the above described methods are summarized in Figure 5.9. Next, we have to determine which of the time steps causes a major change in the spatial variation of deformation (either activity or shortening rate), defining a significant deformation stage for the orogen. The different results are alternately coloured dark grey and light grey, and each of these “stage” changes are marked with a stippled yellow line.

Time steps (1 Ma to the next 1 Ma) for which more than three stippled yellow lines are present are further investigated in the sensitivity analysis. Following the sensitivity analysis described below, the “significant” time windows are highlighted by a through-going solid yellow line; insignificant time steps are marked by a through-going yellow stippled line.

We evaluated the boundaries between two consecutive time steps according to the following impact factor: ($points_{changed}$ *10 / $points_{active}$) / (12 - $areas_{active}$) including the number of changed points from one time step to the next, the number of active points, and the number of active areas. This formula is designed to equally weight these factors, so that significant time windows occur only when a critical amount of active points and active areas changes. For example, when only one or two big areas are active in the first 1 Ma (i.e., data from one or two different authors) and change, then a lot of points are active that can change, but the error can be comparatively large when the original

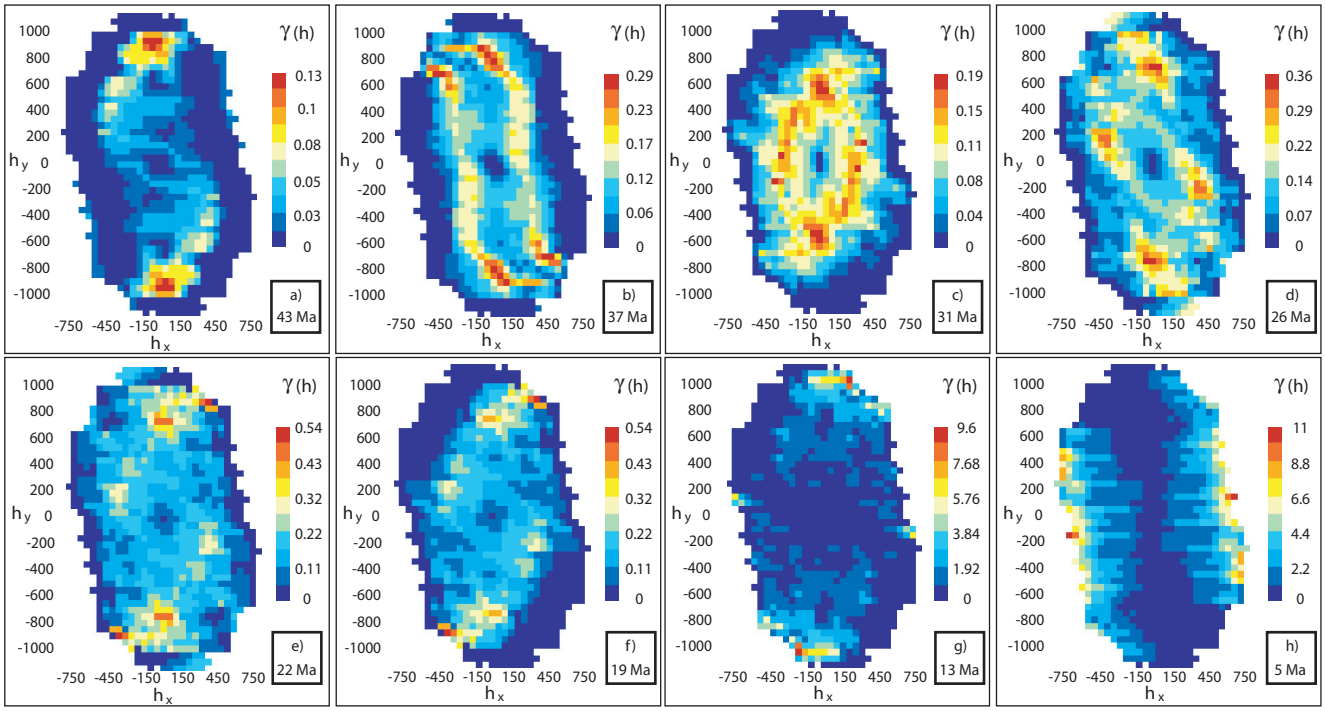

Fig. 5.8: Each of the eight plots a) to h) shows a variogram surface depicting the variation of shortening rates in space. Further description of each plot in-text.

data have an error. On the other hand, when a lot of active areas change but only a small number of points, because the areas are small, it can still be a significant change.

We allowed one additional Ma in our calculation to account for the general area that might result from the original data (e.g., some dating errors do not allow pinpointing deformation with an accuracy of 1 Ma). The result of the impact formula yields values between 0.8 and 9. When they are above 1, we define the stage to be significant. If the value is <1, it is not. Results of the sensitivity analysis are summarized in Appendix A.

5.5.2. Summary

The following deformation time windows appear to be significant with characteristic associated lengths of active structures/ areas, which take the oroclinal bend into account:

1) 46-43 Ma (the Western Cordillera starts to deform), 90 km width and 200 km length;
2) 42-41 Ma (the Eastern Cordillera becomes active), 200 km width and 200 km to 800 km length;
3) 40-34 Ma (the shortening rates of the active areas increase), also 200 km width and 200 km to 800 km length;
4) 33-29 Ma (activity in the Altiplano area begins), 400 km in width and ~400 km in length;
5) 28-18 Ma (more points become active especially in the Eastern Cordillera, but generally local fluctuations of strain distribution occur), 180 km to 270 km in width and 240 km to 800 km in length (up to 21 Ma);
6) 17-13 Ma (the system prepares for a general change in location of strain accumulation), 150 to 200 km in width and 270 km to 800 km in length (already starting from 20 Ma on);
7) 12-11 Ma (the Eastern Cordillera ceases activity, and strain transfers to the Interandean), 150-200 km in width and 400 km to 800 km in length;
8) 10-9 Ma (activity in the Interandean becomes less, but takes up in the Subandean), 100-200 km in width and 270 km to 800-1000 km in length;
9) 8-0 Ma (Subandean shortening remains active until now), 150-200 km but also more than 200 km in width and 300 km to 800-1000 km in length.

In general, the numbers given for the length mean that the two values (minimum and maximum) co-exist, but no values in between the estimates. It seems as if two characteristic lengths exist for the along-strike extents of active areas (namely about 200-300 km for the smaller extent and 600 km for

the large extent up to 800-1000 km when taking the oroclinal bend into account), whereas the width generally yields an estimate of 150-200 km (with deviations of 90 km and up to 270 km). The only exception from these values is the time from 33-29 Ma in which deformation is limited to a rather central cluster that has similar extents along-strike of the units and orthogonal to it.

This allows the conclusion that the width of the active units generally is about 20-50% of the length of active units. The longer length values are 2-5 times the smaller length values. This further suggests that the smaller of the values reflects the extent of a single active area, whereas the larger value represents several active areas, that are coevally active, spatial neighbours. This also explains that the first stage has a width that is half of the common value of stage 2 and stages thereafter, as in the initial time window, no coeval areas seem to have been active, which only begins in the later time windows. The same is true for the along-strike extent, which only yields a value of 200 km, i.e., the length of one active area. A multiple of this length occurs only from the second stage on. However, another difference is striking: before the time of 33-29 Ma in which the plateau interior is active, the common length scale of one area was closer to 200 km, which extents more to 300 km in the time windows after 33-29 Ma.

The characteristic lengths for structures of ~200 km and multiples

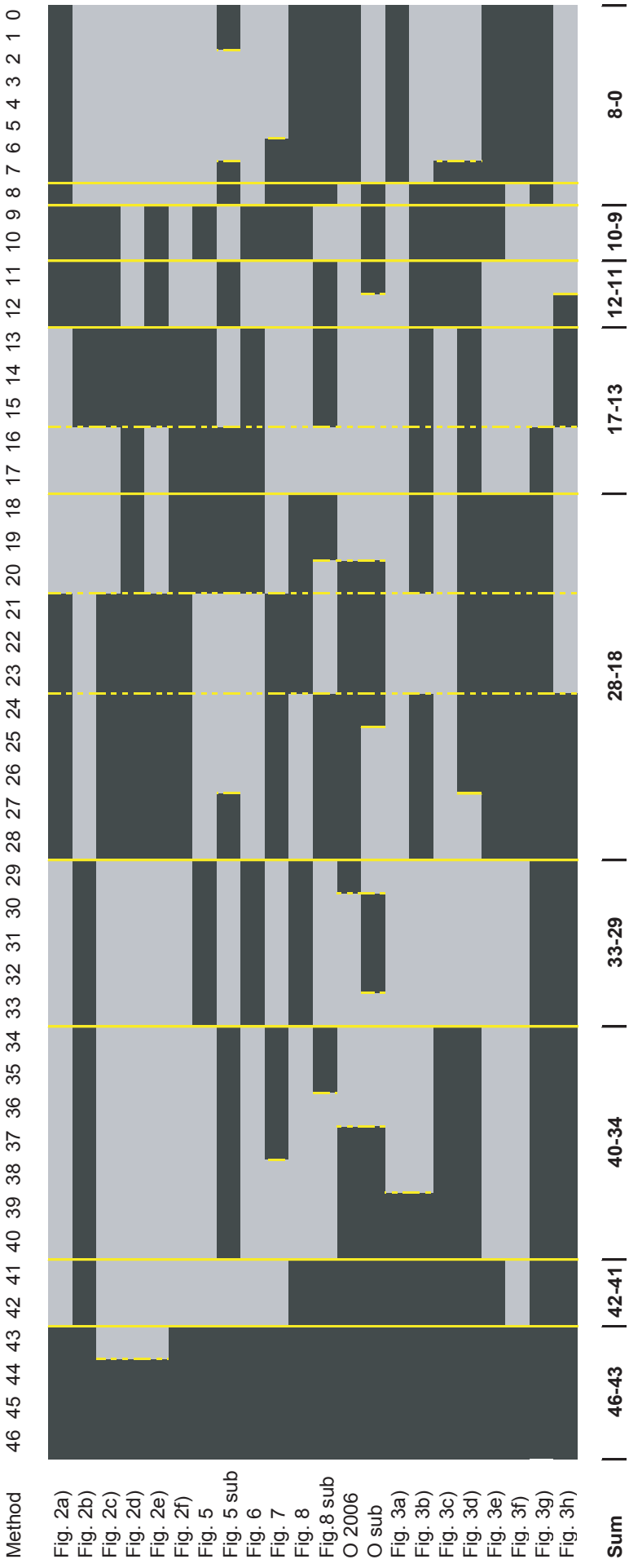

Fig. 5.9: This table is a summary of all deformation stages inferred from the different methods (frequency statistics (Fig. 5.2), indicator variogram surfaces (Fig. 5.5) with substages (termed "Fig. 5.5 sub", not depicted), variograms (Fig. 5.6), kriging plots (Fig. 7), variogram surfaces of shortening rate (Fig. 5.8) and substages (termed "Fig. 5.8 sub", not depicted), deformation periods from Oncken et al. (O 2006) with substages ("O sub"), and more data from frequency statistics (Fig. 5.3). The solid yellow lines indicate major deformation changes over time (from one Ma to the next), whose results are significant, whereas the stippled yellow lines mark stages that are not significant and could rather be interpreted as substages. The row at the bottom shows the resulting deformation time windows when summarized.

thereof suggest that the common structures, e.g., faults in a fault network, have the same scale lengths, irrespective of their position within a structural unit. Each of these smaller areas, probably representing fault systems, can be regarded as a coherent unit, which is independent at first. Their eventual coeval activity causes the multiple lengths (i.e., the larger values) maybe due to an interlinkage between faults. The only exception is the plateau interior: the characteristic length only grows up to ~400 km maximum length.

5.5.3. Discussion

By means of frequency- and geostatistics we studied the spatial pattern of deformation for the Central Andes over the last 46 Ma. By resolving these data down to one million year steps, we are able to detect significant temporal deformation patterns: each deformation stage lasts between 3 and 10 Ma. We have to note that we would not be able to resolve stages below the duration of or with a greater accuracy than 1 Ma, as the error for dating deformation in the initial data is on the order of 1 Ma. All of these stages are driven by the deformation activity in regional areas, which are much smaller in spatial extent than the orogen itself. Thus, the deformation pattern we detect on the orogen scale is solely driven by variations on the next smaller scale, which imprints its effect on the orogen scale.

The smaller scale variations occur on temporal scales that are shorter than some of the deformation stages of the orogen scale mentioned above, namely on the order of 2-4 Ma. Such variations can certainly be ascribed to the different fault systems or faults that are active, to strain transfer between systems and faults, and also to changes in strain accumulation mode. Characteristic lengths of structures for the respective time windows are summarized above, yielding average extents of 150-200 km in width and 200-300 km for along-strike length. When neighbouring structures are coevally active, the characteristic along-strike length increases by a multiple of the characteristic length of one active area, up to 600-800 km (and even 1000 km), as the faults of the smaller scales interconnect.

The shortening rates that we calculate are very small (cf. mean values in Fig. 5.2, 5.3, and 5.4), unlike commonly used values for the past (5-15 mm/yr, e.g., Klosko et al., 2002; Liu et al., 2002). Certainly, our values are minimum estimates (sometimes below mm/yr) and probably not realistic, when compared to other local estimates (1-8 mm/yr, e.g., Elger et al., 2005) as they are calculated under the assumption that strain was distributed homogeneously over the entire area and over time. Thus, as the resulting data are actually “too” low, we could therefore in turn infer and conclude that accumulation of fault slip must be heterogeneous in space and time.

Unfortunately, attributing strain rates for an entire orogen and dividing the formation of an orogen in phases of up to 15-20 Ma during which the entire orogen was actively deforming is often our only option when studying the deformation history of orogens, as better resolved data -both in space and time- are usually not available (due to lack of field exposure).

Strain accumulation exhibits characteristic spatial and temporal structures on the orogen and the next smaller regional scale, and higher data resolution on all scales is needed for the deduction of deformation processes. However, we can compare the regional scale of ~150-200 km in width and 200-300 km in length to the orogen scale pattern which yields up to five times the amount of the length, whereas the width remains about the same. These characteristic scale lengths are the same for all significant time windows, which are themselves commonly on the order of 2-4 Ma, but also twice as much. It remains to be analyzed if the characteristic lengths on the regional scale are real or due to the lack of data resolution below the regional scale. Thus, within the regional area, some parts might actually be inactive, dividing the larger regional area into smaller areas. The characteristic regional scale length would again be merely a summary of lengths found on the smaller scale. Chapter 9 discusses such artefacts resulting from lack of resolution and their implications that strain accumulation can still be scale-invariant.

Characteristic sedimentary sequences, i.e., temporal patterns, have also been suggested for erosional responses to deformation cycles, which are on the order of 2-3 Ma as inferred from sedimentary basin infill in the Central Andes (Elger, 2003; Echavarria et al., 2003); therefore similar to our results for strain accumulation on the regional (fault system) scale.

5.6. Conclusions

With a multitude of both frequency and geostatistics of deformation activity and shortening rates, we examined the spatial strain accumulation pattern on the orogen scale for the last 46 Ma of Central Andean plateau formation, with the goal to identify characteristic temporal and spatial scale lengths on the regional and the orogen scale. We observe the unsystematic way of strain accumulation for the Central Andean plateau orogen, which is in contrast to strain propagation inherent to fold-and-thrust belts.

We were able to calculate shortening rates that are resolved down to a spatial scale of 40 km for time steps of one million year within an orogen of several hundred kilometers extent. The rates are simplified due to the assumption that strain is distributed homogeneously, and therefore merely represent minimum estimates. As they are very low, we propose that strain accumulation does not occur in a homogeneous but a heterogeneous fashion, and varies from one fault system or fault to another. Also, strain accumulation is not continuous over time, but follows a temporal deformation pattern (probably with varying deformation intensities and resulting shortening). As previously suggested by Oncken et al. (2006), these deformation times do not always pertain to along-strike coeval activity, but exhibit regional scale events (2-4 Ma duration). When analyzing deformation activity, these regional scale events have typical scale length of 200-300 km in along-strike extent and 150-200 km in width. As several of these regional areas are active at the same time, the along-strike extent increases to a multiple on the orogen scale, i.e., up to 600-1000 km (cf. Chapter 9 for further discussion).

Most of the regional deformation stages on the order of 2-4 Ma significantly affect the orogen scale pattern, so that we propose the following main deformational stages for the Central Andean plateau: 46-43 Ma, 42-41 Ma, 40-34 Ma, 33-29 Ma, 28-18 Ma, 17-13 Ma, 12-11 Ma, 10-9 Ma, and 8-0 Ma.

Acknowledgments

This work is part of KS' PhD thesis, funded by a stipend from the "Studienstiftung des deutschen Volkes" (National Merit Foundation). Martina Böhme double-checked the accuracy of the data and helped with the preparation of figures and diagrams.